

**Online Deposit**

**High-precision oxygen isotope analysis of picogram samples reveals 2 $\mu$ m gradients and slow diffusion in zircon**

**Fig. D1 CL images of zircon and SE images of ion microprobe pits: Surface 2**

Daniel's Road melanosome

Sample IP360, BMH-04-01a zircon 35

Analysis numbers correspond to those found in Table D1

Analyses with irregular pits (on cracks) are indicated with an asterisk.

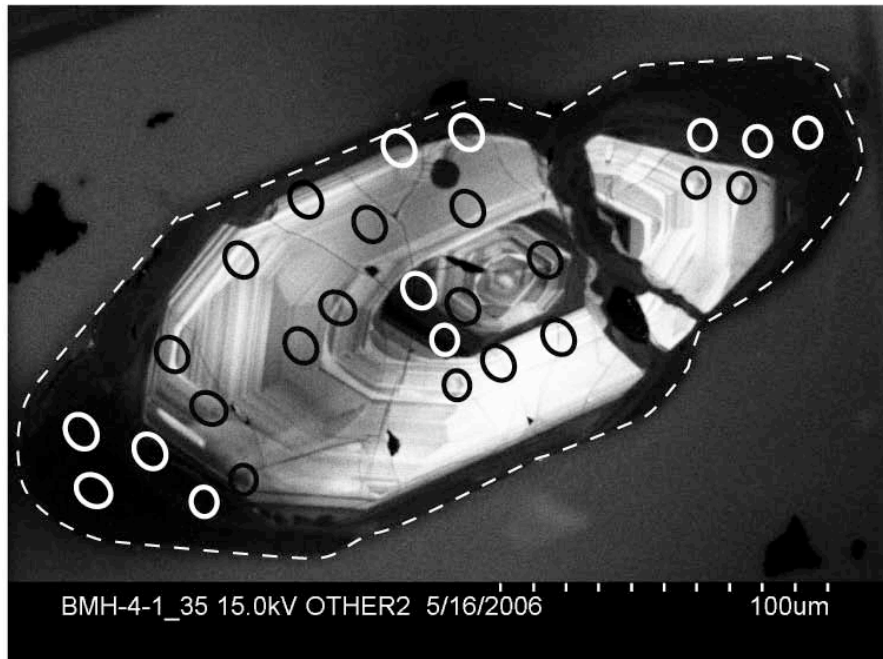
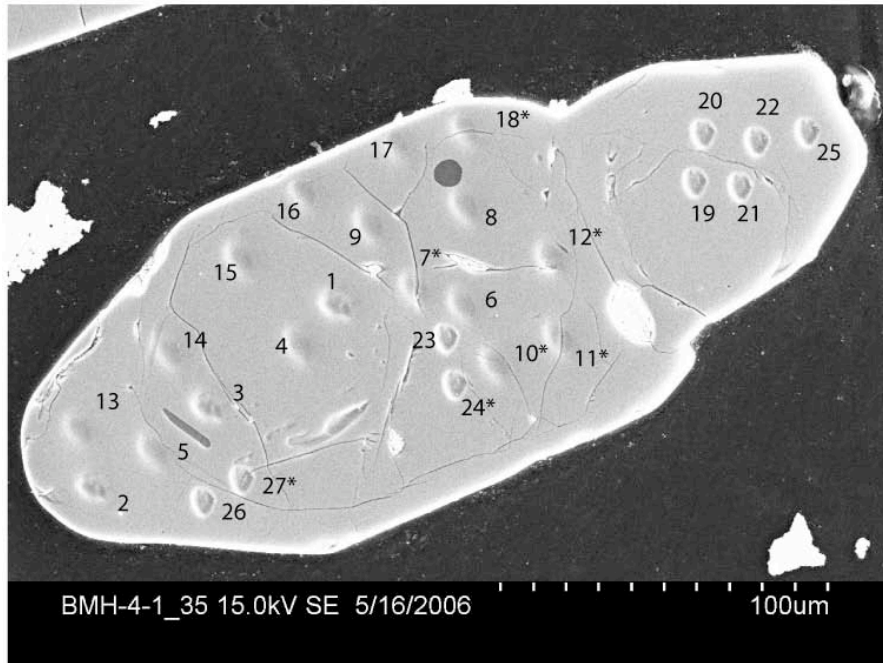
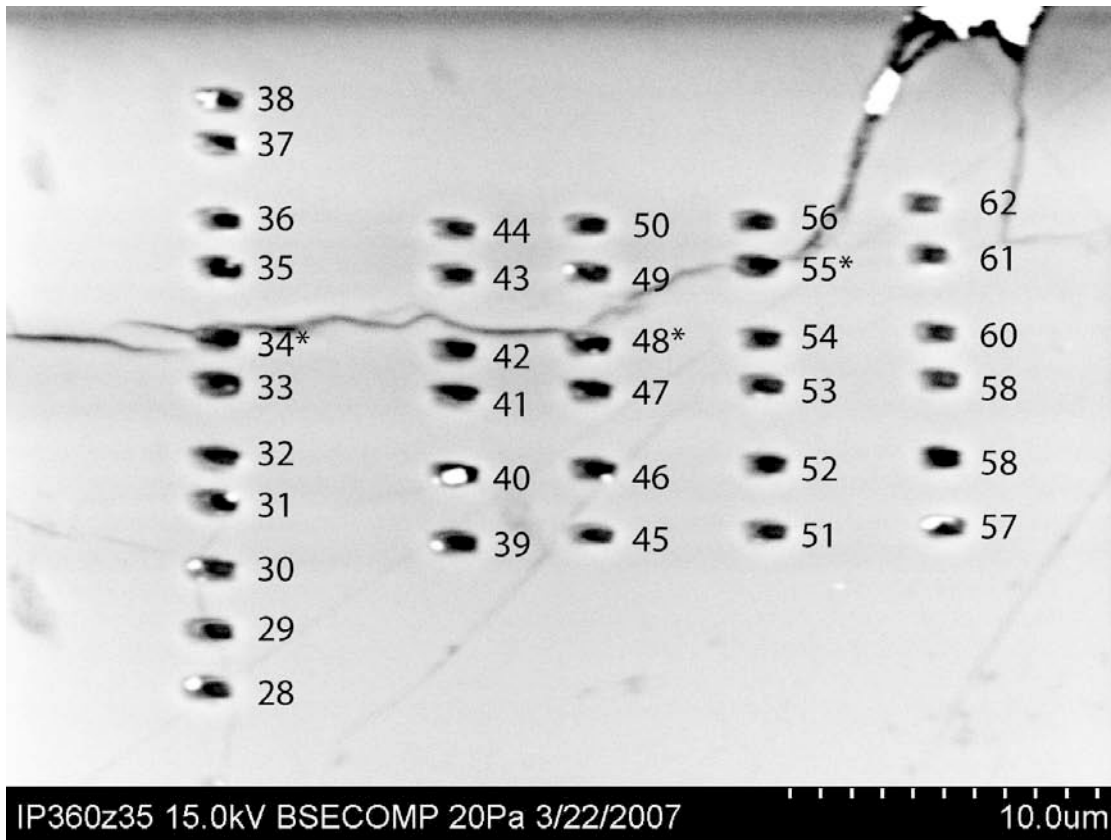


Fig. D2 CL images of zircon and SE images of ion microprobe pits: Surface 3



### **Analytical Methods: 7 $\mu$ m and 10 $\mu$ m analyses**

Oxygen isotopic analyses were performed on the Wisc-SIMS CAMECA ims-1280 high-resolution, multi-collector ion microprobe at the University of Wisconsin – Madison in 3 analytical sessions using 10 or 7  $\mu$ m spots size (Sessions 1-3 in Table D1). A  $^{133}\text{Cs}^+$  primary ion beam (20 keV total acceleration voltage) was focused to a diameter of 7 or 10  $\mu$ m (depending on analysis session) on the sample surface. Secondary  $\text{O}^-$  ions were accelerated away from the sample by  $-10$  kV and the analysis site was centered under a uniform electron field generated by a normal-incidence electron gun for charge compensation. Primary ion intensities were ca. 1 nA (7  $\mu$ m primary beam) or ca. 1-2 nA (10  $\mu$ m primary beam). The secondary optics were configured similarly to those reported in Kita et al. (2007) and aim to achieve high secondary ion transmission. Instrument parameters include: transfer lens magnification of 200, contrast aperture (CA) 400  $\mu$ m diameter, field aperture (FA) 4000 x 4000  $\mu$ m square, entrance slit 122  $\mu$ m width, energy slit 40 eV width, and exit slit width 500 $\mu$ m. At these conditions, both the primary ion spot images transferred to the FA window and the crossover images through the CA and entrance slit were almost fully transmitted. The intensity of  $^{16}\text{O}$  was (1-2)  $\times 10^9$  cps depending on the primary intensity (ca.  $10^9$  cps/nA). Mass resolving power (MRP) was set to ca. 2500, enough to separate hydride interferences on  $^{18}\text{O}$ . Two multi-collector Faraday Cups (FC) were used to measure  $^{16}\text{O}$  and  $^{18}\text{O}$  simultaneously, equipped with different amplifiers ( $10^{10}$  and  $10^{11}$   $\Omega$  resistors, respectively). The base line of the FC amplifiers was calibrated at the beginning of each analytical session; drift during the day was insignificant compared to the noise level of the detectors ( $\leq 1000$  cps for FC with  $10^{11}$   $\Omega$  resistor). The magnetic field was regulated by a Nuclear Magnetic Resonance (NMR) probe with stability of mass better than 10 ppm/10 hours. At each analysis position, any small misalignment of the secondary optics due to changing stage position

was automatically re-tuned before each analysis. Total analytical time per spot was about 4 min, including time for locating and selecting the analytical positions (1 – 2 min), pre-sputtering (10 sec), automatic retuning of the secondary beam (ca. 60 sec), and analysis (80 sec). Data were corrected for instrumental mass fractionation (IMF) using fragments of the zircon standard KIM-5 mounted in each sample block (Valley 2003; Cavosie et al. 2005). Standards were measured ca. four times every 10-20 sample analyses and the average value of IMF of the standard analyses that bracket the sample analyses was used as IMF correction. The external errors of bracketing standard analyses were 0.3-0.4‰ (2 S.D.) for 10 $\mu$ m analyses, and 0.7 ‰ (2 S.D.) for 7  $\mu$ m analyses, and represent the spot to spot precision of this technique.

#### **Analytical Methods – sub-1 $\mu$ m analyses**

Three sessions of sub-1 $\mu$ m analyses were performed (Sessions 4-6, Table D1) with the instrument configured as above with the following exceptions. The beam was focused to smaller than 1  $\mu$ m, confirmed by imaging of a calibrated Si wafer. Because ion probe pits are generally longer in the X-direction (in the plane of both the primary and secondary ion beams) the sample was inserted so that planned traverses would be in the Y-direction, allowing for the highest spatial resolution. Secondary electron images of the pits show pit dimensions of 600 nm x 900 nm with a shallow halo of  $\sim$ 1.5 x 2  $\mu$ m due to primary beam aberration. The intensity of  $^{16}\text{O}$  was (1-2) x10<sup>6</sup> cps, depending on the primary beam intensity, which ranged from 2 to 1 pA over the analytical sessions.  $^{18}\text{O}$  was measured using a miniaturized Hamamatsu electron multiplier (EM) in the multicollector. The dead time of the detector is estimated to be 68ns, which is very close to the hardware setting of the counting system. The pulse height distribution of the EM detector was adjusted to peak at 280mV before the KIM5 standard analyses and was not changed during the session because relatively lower  $^{18}\text{O}$  ion currents (2,000-4,000 cps) are unlikely to cause

aging of the EM detector during a single day of analyses. The use of an EM/FC configuration for these analyses results in rather different raw  $\delta^{18}\text{O}$  values than those measured using the FC/FC configuration of the 7 and 10  $\mu\text{m}$  analyses as would be predicted based on the different properties of these detectors. Total analytical time per spot was about 24 minutes including pre-sputtering (360 sec), automatic retuning of the secondary beam (ca. 60 sec), and analysis (1000 sec). One analysis pit made with an estimated primary beam intensity of 1.8 pA (based on  $10^9$  cps of  $^{16}\text{O}$  per nA) was cut in cross section parallel to its long axis using a Zeiss Crossbeam Focused Ion Beam (FIB) instrument (Fig. D3). The depth of this pit was measured as 1.0  $\mu\text{m}$ . Estimated primary beam intensities for sub-1 $\mu\text{m}$  analyses of 1-1.9 pA yield pit depths of 0.6 to 1.1  $\mu\text{m}$ .

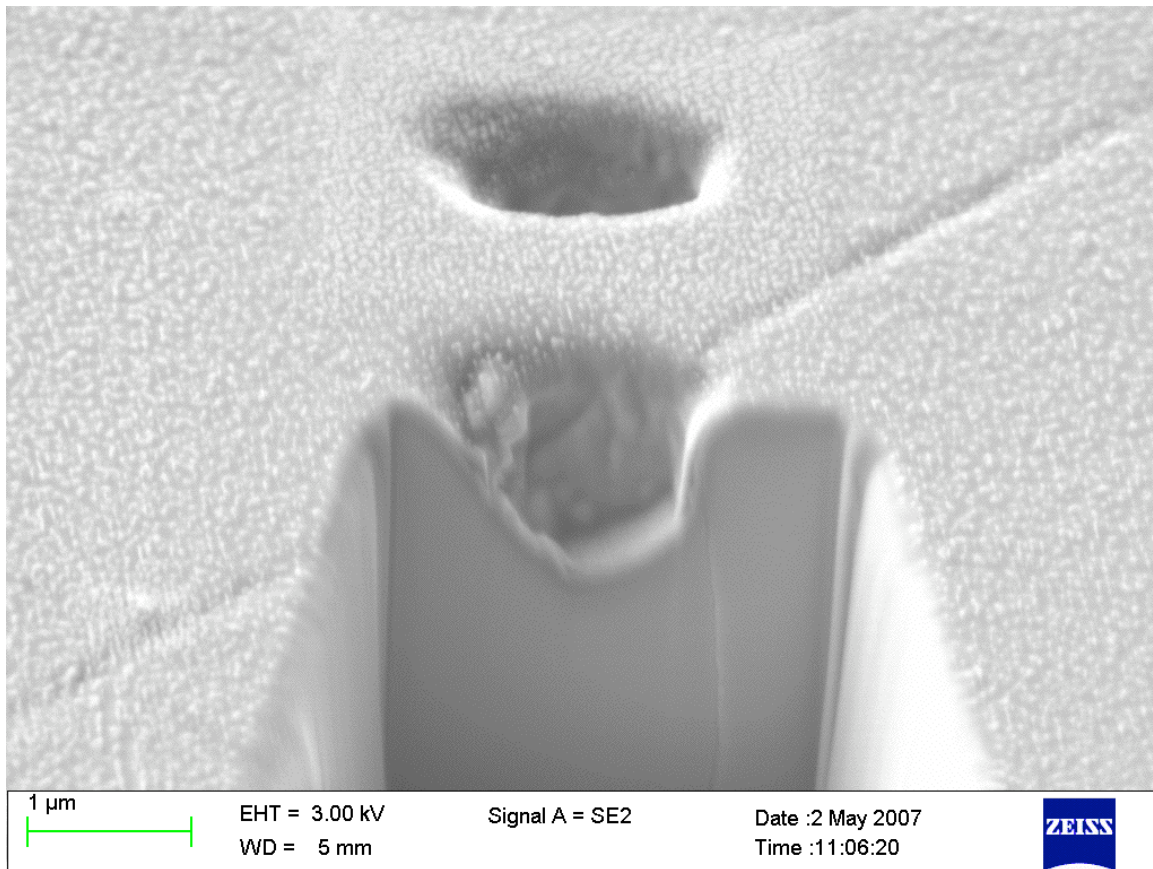


Fig. D3 Oblique SE image of a pit cross-sectioned using a focused ion beam. Pit depth is  $\sim 1\mu\text{m}$ .

Analyses of the Adirondack zircon were performed in 5 traverses normal to the boundary of igneous core and metamorphic overgrowth (in the Y direction of the stage). The first traverse was of 11 analyses each ~2  $\mu\text{m}$  apart. Once it was clear that analyses were in the correct region of the zircon (pits were barely visible in the reflected light system) four additional traverses of 6 analyses were made. Regular analyses of the standard KIM-5 were not made during this analysis session because it was unclear whether the stage would return to the analysis position correctly after moving to the standard position. Analyses were corrected for IMF by normalizing the average of all rim analyses farther than 2.5  $\mu\text{m}$  from the CL boundary to the average rim composition of 12.7‰ VSMOW defined by the average of all 7 and 10  $\mu\text{m}$  rim analyses greater than one pit radius from the CL boundary. Precision was estimated using seven analyses of the KIM-5 standard in a different sample mount (WI-STD-9) in Session 4, and six analyses of KIM-5 in Session 6 performed immediately before and after the Adirondack zircon analyses of Session 5. No systematic drift of the measured ratios occurred before and after sample analyses. Reproducibility of the 13 analyses of KIM-5 from the two bracketing sessions is 2.0‰ (2 S.D.). Samples were not corrected for IMF using KIM-5 because in this case it was on a different sample block.

## References

- Cavosie, A.J., Valley, J.W., Wilde, S.A., and EIMF. (2005) Magmatic  $\delta^{18}\text{O}$  in 4400–3900 Ma detrital zircons: A record of the alteration and recycling of crust in the Early Archean. *Earth and Planetary Science Letters*, 235, 663-681.
- Kita, N.T., Ushikubo, T., Fu, B., Spicuzza, M.J., and Valley, J.W. (2007) Analytical developments on oxygen three isotope analyses using a new generation ion microprobe ims-1280. *Lunar and Planetary Science*, XXXVIII, Abstract 1981.

Valley, J.W. (2003) Oxygen isotopes in zircon. In J.M. Hanchar, and P.W.O. Hoskin, Eds.  
Zircon, Reviews in Mineralogy & Geochemistry v.53, p. 343-385. Mineralogical Society  
of America/Geochemical Society, Washington, DC.

Table D1. Oxygen isotope analyses by ion microprobe of the Daniel's Road Adirondack zircon

Pit number	distance from		$^{16}\text{O}$ cps $\times 10^6$	$\delta^{18}\text{O}$ raw	$\delta^{18}\text{O}$ VSMOW	$2\sigma$ ††
	boundary†	$\mu\text{m}$				
Session 1, 10 $\mu\text{m}$ pit, Feb. 2006						
KIM-5			2005	7.4		
KIM-5			1999	7.4		
KIM-5			2010	7.6		
KIM-5			2003	7.5		
1	-33		1967	7.8	5.2	0.3
2	20		1976	14.8	12.3	0.3
3	-15		1963	7.5	4.9	0.3
KIM-5			1958	7.2		
KIM-5			1950	7.3		
KIM-5			1944	7.1		
KIM-5			1950	7.5		
Session 2, 10 $\mu\text{m}$ pit, March 2006						
KIM-5			1902	7.9		
KIM-5			1890	7.6		
KIM-5			1857	7.8		
KIM-5			1855	7.7		
4	-40		1821	8.3	5.8	0.4
5	5		1836	14.8	12.3	0.4
6	-40		1806	9.6	7.1	0.4
7*	-40		1819	11.3	8.8	0.4
8	-20		1802	8.5	6.0	0.4
9	-18		1808	8.6	6.1	0.4
10*	-22		1797	8.9	6.4	0.4
11*	-22		1769	8.4	5.9	0.4
12*	-8		1767	8.1	5.6	0.4
13	20		1773	14.8	12.4	0.4
14	-5		1884	8.4	5.9	0.4
15	-9		2053	7.9	5.4	0.4
16	0		2011	10.4	7.9	0.4
17	2		1960	12.2	9.8	0.4
18*	2		1897	13.5	11.0	0.4
KIM-5			2134	7.4		
KIM-5			2028	7.3		
KIM-5			1968	7.7		
KIM-5			1943	7.4		
KIM-5			1917	7.5		

†Distance measured on SE/CL composite image, negative numbers indicate core analyses

††2 S.D. of the bracketing standard analyses.

\* Analysis made on a crack, discarded as irregular



Table D1 cont'd. Oxygen isotope analyses by ion microprobe of the Daniel's Road Adirondack zircon

Pit number	distance from		$^{16}\text{O}$ cps $\times 10^6$	$\delta^{18}\text{O}$ raw	$\delta^{18}\text{O}$ VSMOW	$2\sigma$ ††
	boundary†	$\mu\text{m}$				
Session 3, 7 $\mu\text{m}$ pit, May 2006						
KIM-5			923	6.9		
KIM-5			931	6.8		
KIM-5			926	6.9		
KIM-5			925	7.3		
19	-6		931	7.6	5.5	0.7
20	7		920	15.8	13.6	0.7
21	-5		931	7.4	5.3	0.7
22	9		930	15.0	12.9	0.7
23	-37		912	12.7	10.5	0.7
24*	-24*		904	7.7	5.6	0.7
25	20		958	13.9	11.7	0.7
26	7		844	15.3	13.2	0.7
27*	5		917	6.8	4.7	0.7
KIM-5			901	7.5		
KIM-5			916	7.1		
KIM-5			891	7.8		
KIM-5			907	7.4		

†Distance measured on SE/CL composite image, negative numbers indicate core analyses

††2 S.D. of the bracketing standard analyses.

\* Analysis made on a crack, discarded as irregular

Table D1 cont'd. Oxygen isotope analyses by ion microprobe of the Daniel's Road Adirondack zircon

Pit number	distance from		$^{16}\text{O}$ cps $\times 10^6$	$\delta^{18}\text{O}$ raw	$\delta^{18}\text{O}$ VSMOW	$2\sigma$ ††
	boundary†	$\mu\text{m}$				
Session 4, sub-1 $\mu\text{m}$ pit, March 2007, Standard Mount†††						
KIM-5			1.92	-1.2		
KIM-5			1.90	0.5		
KIM-5			1.84	-1.2		
KIM-5			1.79	-1.2		
KIM-5			1.82	-1.3		
KIM-5			1.84	-1.8		
KIM-5			1.81	-1.3		
				-1.1 $\pm$ 1.4 Average $\pm$ 2 S.D.		

Session 5, sub-1  $\mu\text{m}$  pit, March 2007, Sample Mount IP 360

Traverse 1

28	rim#	11.5	1.95	4.7	12.4	2.0
29	rim#	9.7	1.91	3.2	10.9	2.0
30	rim#	7.6	1.83	3.1	10.9	2.0
31	rim#	5.5	1.94	4.8	12.5	2.0
32	rim#	4.0	1.82	3.8	11.5	2.0
33	rim	1.7	1.86	4.6	12.4	2.0
34*	rim	0.3	2.00	-3.7	4.0	2.0
35	core	-2.1	1.84	-1.0	6.8	2.0
36	core	-3.8	1.82	-1.6	6.2	2.0
37	core	-6.1	1.80	-2.9	4.9	2.0
38	core	-7.6	1.78	-3.3	4.4	2.0

Traverse 2

39	rim#	7.5	1.76	4.2	12.0	2.0
40	rim#	5.3	1.69	4.7	12.5	2.0
41	rim#	2.6	1.68	3.6	11.3	2.0
42	rim	1.1	1.68	1.0	8.8	2.0
43	core	-1.3	1.57	-2.1	5.7	2.0
44	core	-2.8	1.58	-1.6	6.2	2.0

†Distance measured on SE/CL composite image, negative numbers indicate core analyses

†† 2 S.D. of the bracketing standard analyses.

††† KIM-5 analyses were made on a standard mount and were not used to correct data collected with a sub-1 $\mu\text{m}$  spot.

# Sub-1 $\mu\text{m}$  analyses were standardized to the average rim composition of 12.7 ‰, the average of all 7 and 10  $\mu\text{m}$  analyses > 1 beam radius from core/rim interface. Spots with distance > +2.5  $\mu\text{m}$  from the interface were used for standardization

\* Analysis made on a crack, discarded as irregular

Table D1 concl'd. Oxygen isotope analyses by ion microprobe of the Daniel's Road Adirondack zircon

Pit number		distance from		$^{16}\text{O}$ cps x $10^6$	$\delta^{18}\text{O}$ raw	$\delta^{18}\text{O}$ VSMOW	$2\sigma$ ††
		boundary†	$\mu\text{m}$				
Traverse 3							
45	rim#		7.8	1.53	4.2	12.0	2.0
46	rim#		5.6	1.53	4.5	12.3	2.0
47	rim#		3.0	1.49	4.2	11.9	2.0
48*	rim		1.5	1.37	0.0	7.7	2.0
49	core		-0.7	1.38	0.7	8.4	2.0
50	core		-2.4	1.34	-1.7	6.1	2.0
Traverse 4							
51	rim#		8.0	1.37	4.0	11.7	2.0
52	rim#		5.9	1.30	4.8	12.5	2.0
53	rim#		3.3	1.30	5.6	13.3	2.0
54	rim		1.7	1.28	4.6	12.4	2.0
55*	core		-0.4	1.35	-3.6	4.1	2.0
56	core		-1.9	1.21	-2.1	5.6	2.0
Traverse 5							
57	rim#		8.2	1.15	5.5	13.4	2.0
58	rim#		5.9	1.09	5.0	12.8	2.0
59	rim#		3.3	1.11	5.6	13.4	2.0
60	rim		1.8	1.09	4.2	12.0	2.0
61	core		-0.8	0.98	-3.1	4.6	2.0
62	core		-2.6	1.00	0.1	7.9	2.0

Avg  $\pm$  2 S.D. of zircon rim:  $4.6 \pm 1.6\#$

Session 6, sub-1  $\mu\text{m}$  pit, March 2007, Standard Mount†††

KIM-5	1.14	-1.2
KIM-5	1.11	-2.2
KIM-5	1.09	0.7
KIM-5	1.07	-1.2
KIM-5	0.99	-3.2
KIM-5	1.00	-0.8
	Average $\pm$ 2 S.D.	<u><u><math>-1.3 \pm 2.7</math></u></u>
	Average Sessions 4 & 6 $\pm$ 2 S.D.	$-1.2 \pm 2.0$

† Distance measured on SE/CL composite image, negative numbers indicate core analyses

†† 2 S.D. of the bracketing standard analyses.

††† KIM-5 analyses were made on a standard mount and were not used to correct data collected with a sub-1 $\mu\text{m}$  spot.

#Sub-1 $\mu\text{m}$  analyses were standardized to the average rim composition of 12.7 ‰, the average of all 7 and 10  $\mu\text{m}$  analyses > 1 beam radius from core/rim interface. Spots with distance > +2.5  $\mu\text{m}$  from the interface were used for standardization

\* Analysis made on a crack, discarded as irregular